

Electronic Supplementary Material

Thermoelectric properties of Lead halide Janus layers - A theoretical investigation

A.E. Sudheer ^a, M Vallinayagam ^{b,c}, G Tejaswini ^a, Amrendra Kumar ^{d,e},
M Posselt ^f, C Kamal ^{d,e}, M Zschornak^{*,c,b}, D Murali^{*,a},

^a Department of Sciences, Indian Institute of Information Technology Design and Manufacturing Kurnool
Andhra Pradesh, 518007, India

^b Institute of Experimental Physics, TU Bergakademie Freiberg, Leipziger Str. 23, 09596 Freiberg,
Germany

^c Technical Physics, University of Applied Sciences, Friedrich-List-Platz 1, 01069 Dresden, Germany,
matthias.zschornak@htw-dresden.de

^d Theory and Simulations Laboratory, Theoretical and Computational Physics Section, Raja Ramanna
Centre for Advanced Technology, Indore 452013, India

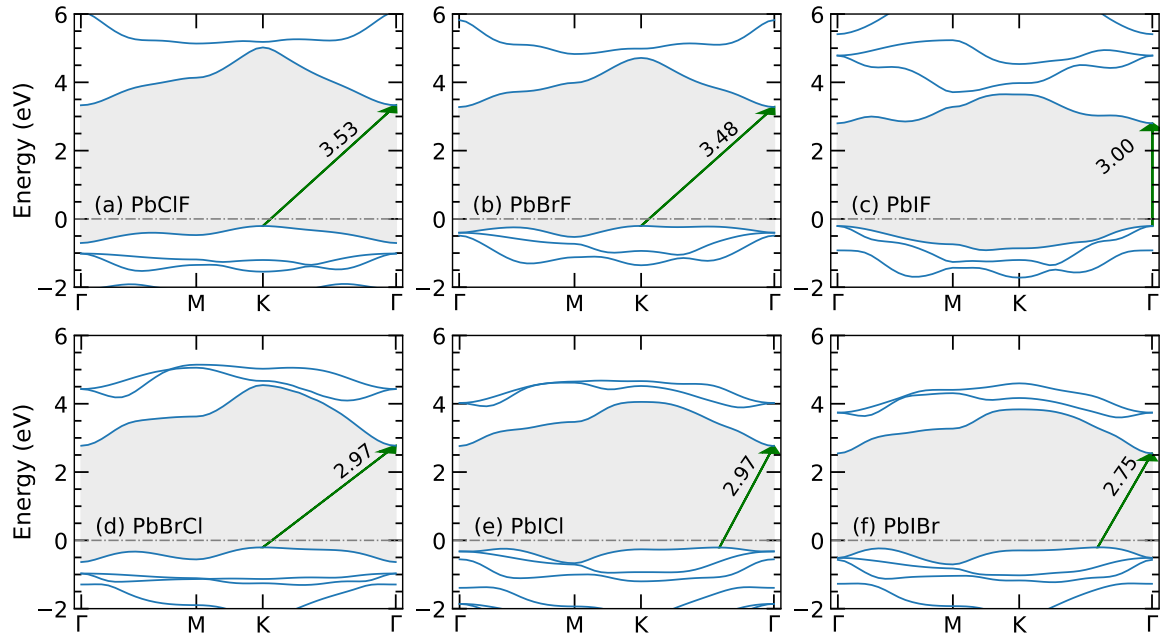
^e Homi Bhabha National Institute, Training School Complex, Mumbai 400094, India

^f Helmholtz-Zentrum Dresden-Rossendorf, Institute of Ion Beam Physics and Materials Research, 01328
Dresden, Germany, dmurali@iiitk.ac.in

Table of Contents

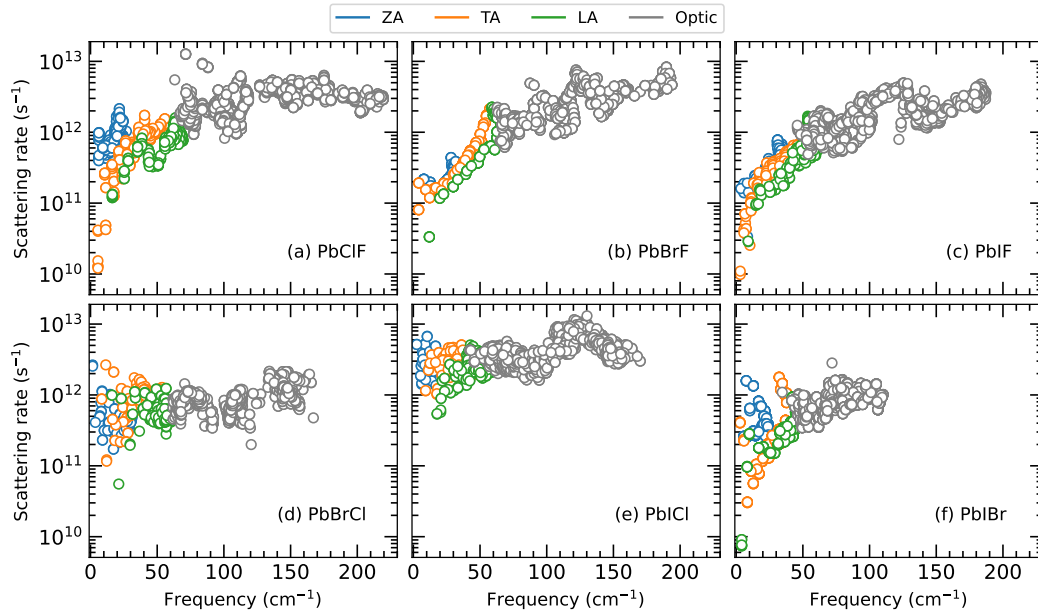
1	Electronic bands	1
2	Phonon Scattering rate	2
3	Phonon group velocity	2
4	Phonon mean free path	3
5	Mobility and Relaxation time	3
6	Phonon band structure	4
7	Calculated parameters from deformation potential approach	5
8	Thermoelectric coefficients of F PbXY Janus layers along armchair direction	6
9	Thermoelectric coefficients of L PbXY Janus layers along arm-chair direction	7
10	Heat-energy conversion efficiency	8

1 Electronic bands



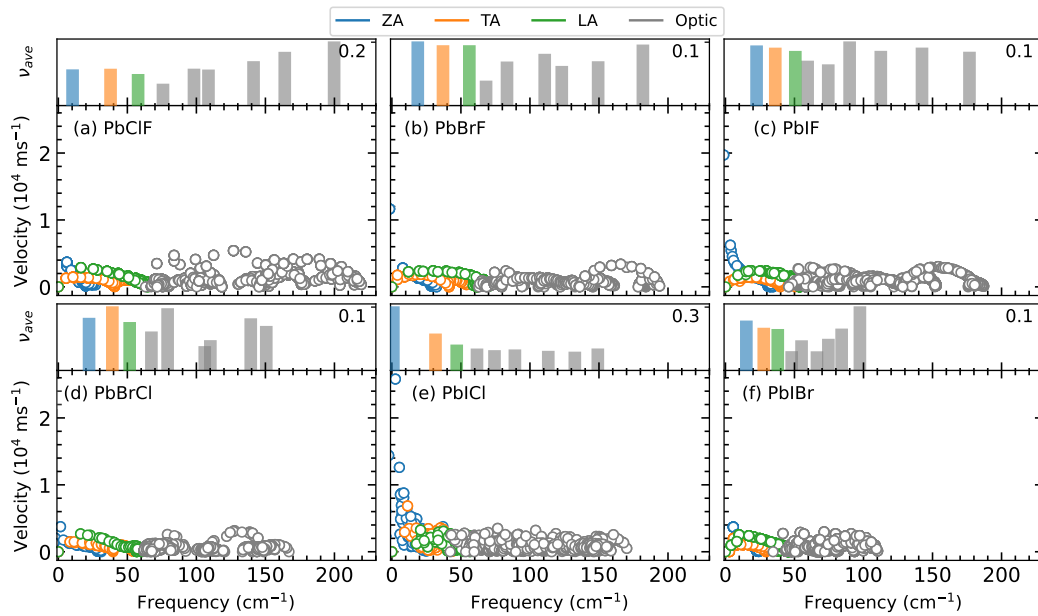
SFig. 1: The energy levels derived from the wavefunction coefficients, calculated using Boltztrap¹. The energy levels agree well with the DFT simulation reported in Ref.². The Fermi level is set at 0 eV, represented by the dashed gray line. The shaded region indicates all possible band gaps between valence and conduction bands. The minimal electronic bandgap is in the $K - \Gamma$ direction, except for PbIF, which is a direct bandgap exactly at Γ . The green arrow guides the visualization of valence (conduction) band minimum (maximum) locations along with the calculated bandgap in eV.

2 Phonon Scattering rate



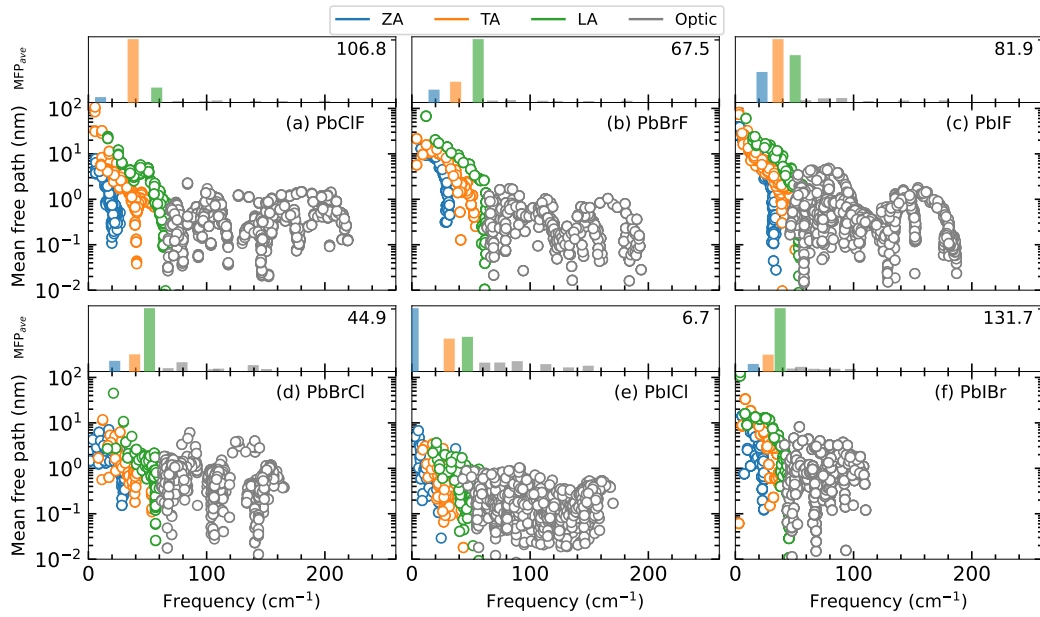
SFig. 2: The mode-resolved phonon scattering rate determined as $\Gamma_\lambda = 1/\tau_\lambda$, where τ_λ is the phonon life time.

3 Phonon group velocity



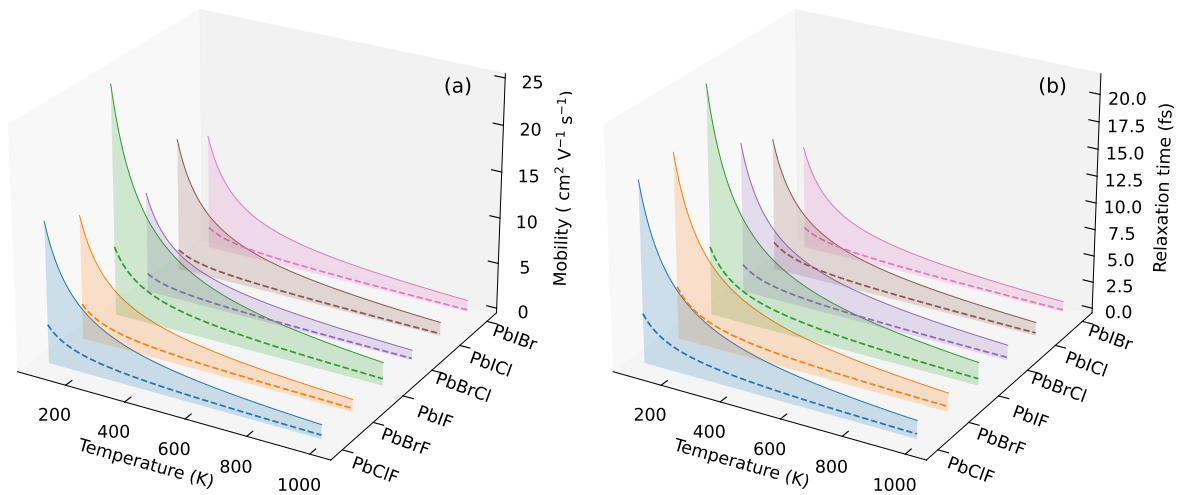
SFig. 3: The mode-resolved phonon group velocity.

4 Phonon mean free path



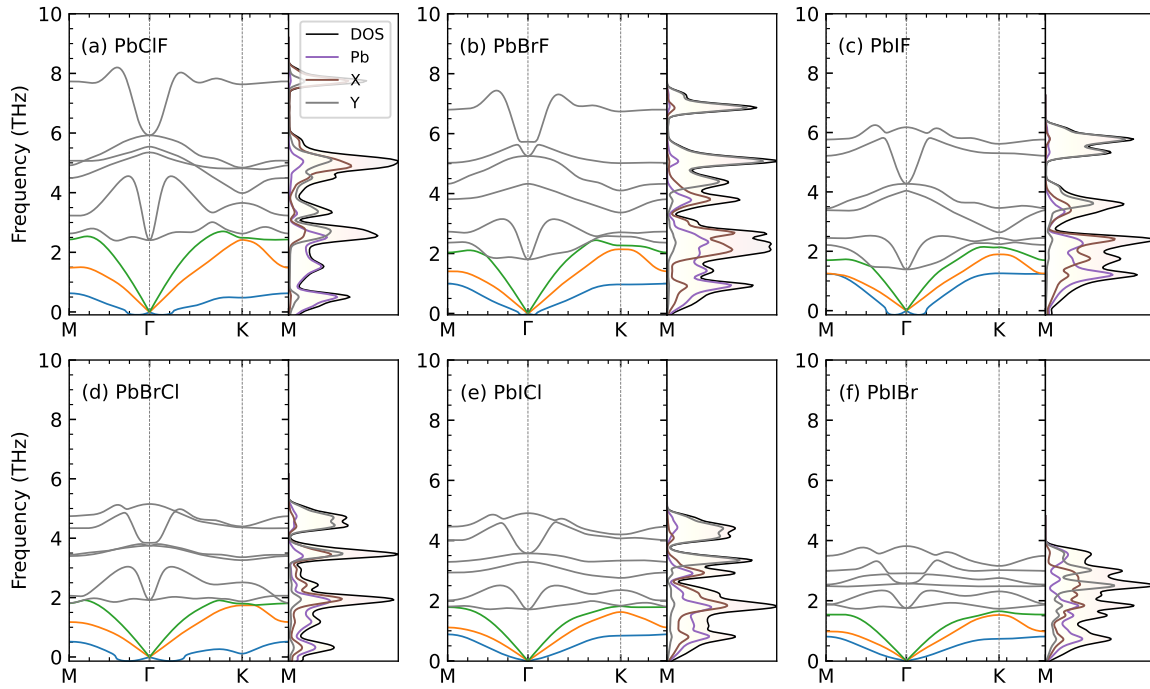
SFig. 4: The mode-resolved phonon mean free path.

5 Mobility and Relaxation time



SFig. 5: The calculated x - and y -components of (a, c) mobility μ and (b, d) corresponding relaxation time τ of holes in PbXY JLs. In mobility of holes along x - and y -directions is, in general, less than that of electrons and relaxes in a shorter period. Therefore, the electrons contribute more to enhancing the TE characteristics than the holes.

6 Phonon band structure



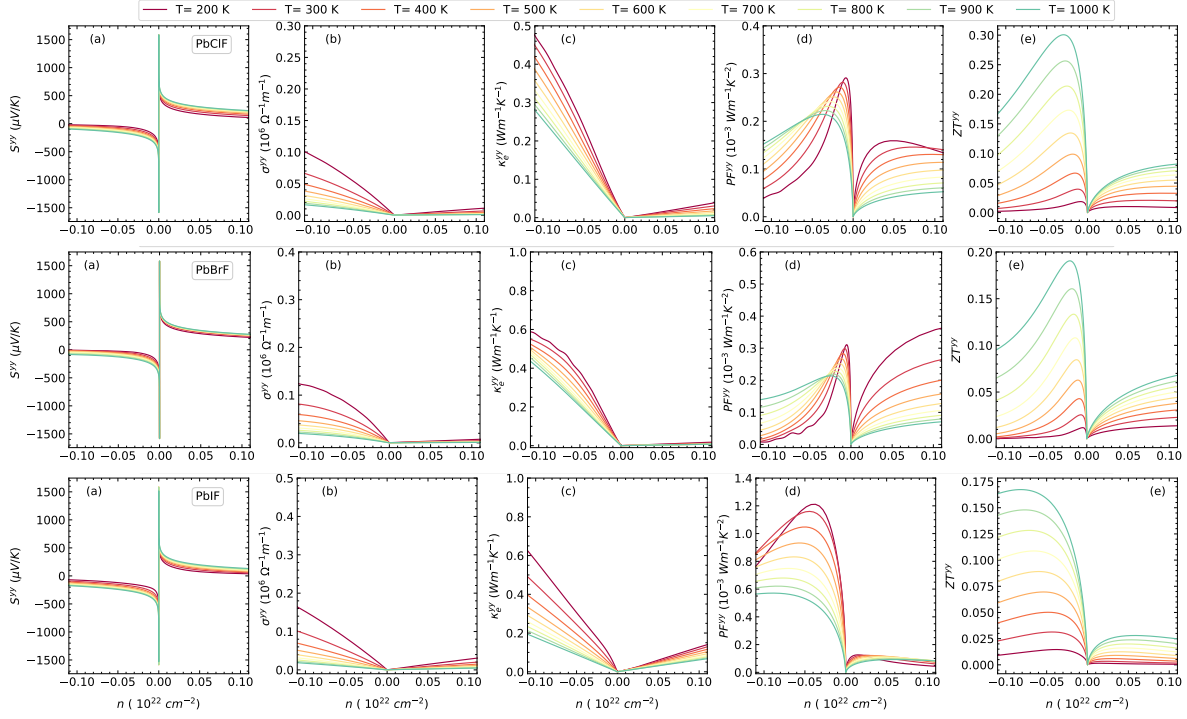
SFig. 6: The calculated phonon band structure of (a-c) F^- - and (d-f) L^- -JLs along with the phonon density of states (DOS). The X and Y symbols in the DOS panel represent the first and second halides in the chemical formula. The colored and gray lines represent the acoustic and optic modes. As the halide atomic weight increases, the vibration frequency range decreases.

7 Calculated parameters from deformation potential approach

Table S1: The calculated elastic modulus C_β in Nm^{-1} , deformation potential constant E_d (eV), electron effective mass m^* in m_e (electron mass), and relaxation time τ in fs of PbXY JLs are presented.

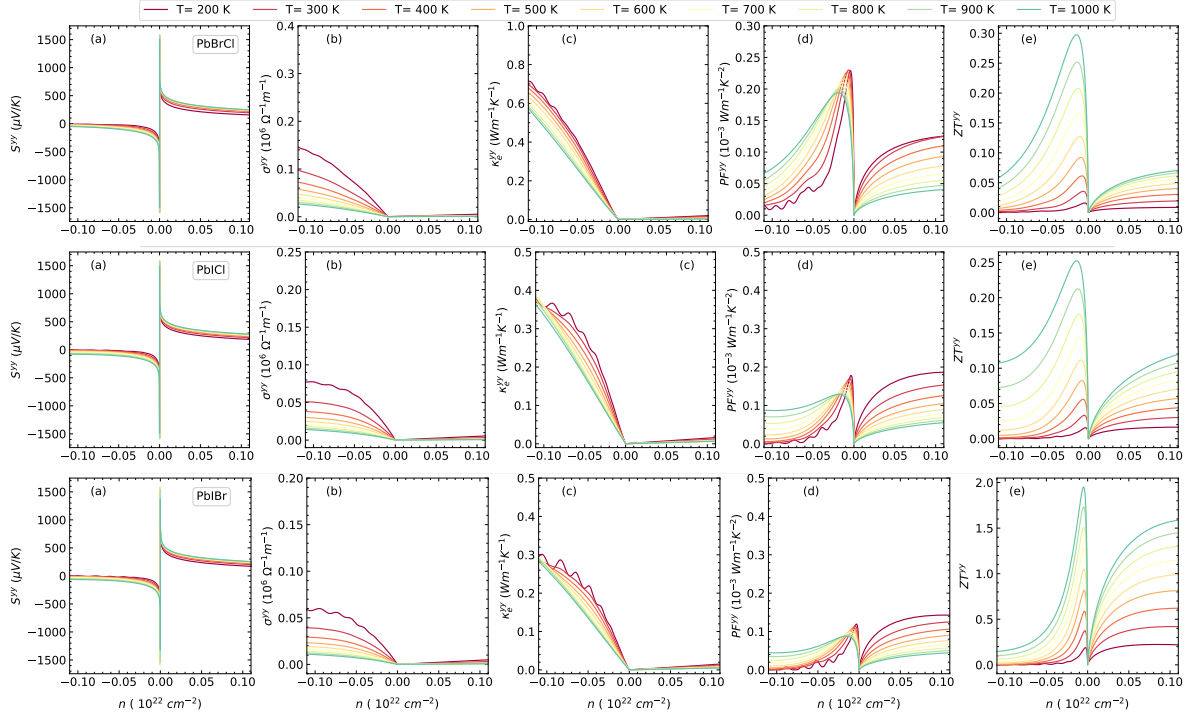
	Direction	C_β (Nm^{-1})	E_d (eV)	m^* (m_e)	
				Electron	Hole
PbClF	x	27.22	3.16	0.591	-1.943
	y	9.99	3.16	0.591	-1.943
PbBrF	x	26.65	3.39	0.469	-2.267
	y	10.26	3.39	0.469	-2.267
PbIF	x	27.07	4.13	0.425	-1.511
	y	10.85	4.13	0.425	-1.511
PbBrCl	x	17.05	2.22	0.331	-2.267
	y	4.51	2.22	0.331	-2.267
PbICl	x	17.48	2.77	0.302	-1.511
	y	4.94	2.77	0.302	-2.093
PbIBr	x	16.60	2.61	0.272	-1.360
	y	4.48	2.61	0.272	-1.511

8 Thermoelectric coefficients of F PbXY Janus layers along armchair direction



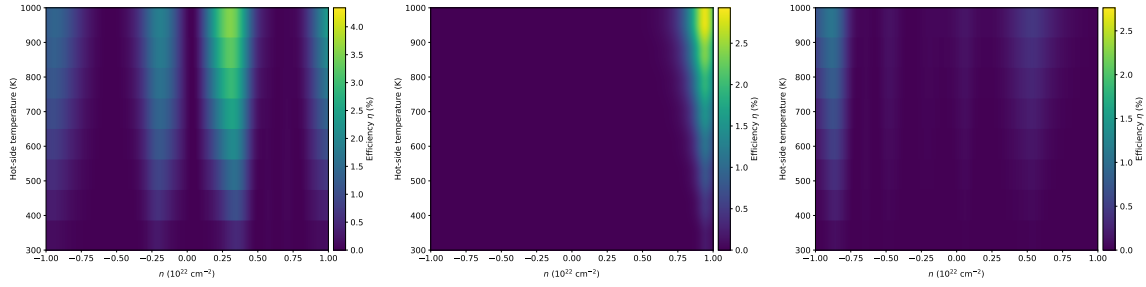
SFig. 7: The calculated yy -components of a) S , b) σ , c) κ_e , d) PF , and e) ZT of PbCIF (top row), PbBrF (middle row), and PbIF (bottom row) JLs with electron relaxation time along armchair (y) direction. The negative (positive) N represents the electron (hole) carrier concentration.

9 Thermoelectric coefficients of L PbXY Janus layers along arm-chair direction

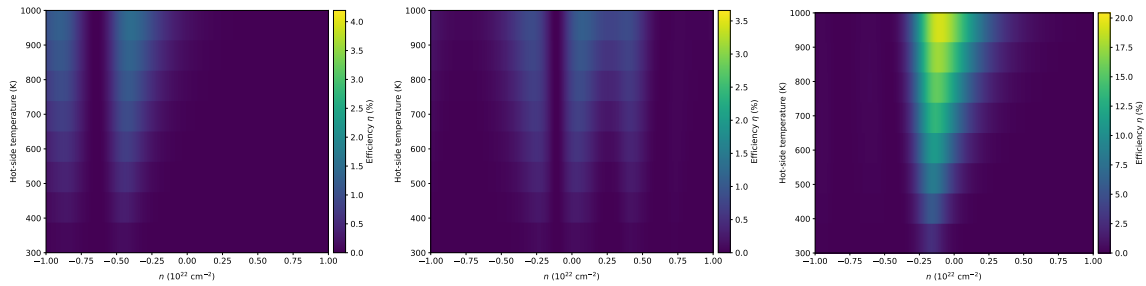


SFig. 8: The calculated yy -components of a) S , b) σ , c) κ_e , d) PF , and e) ZT of PbClF (top row), PbBrF (middle row), and PbIF (bottom row) JLs with electron relaxation time along armchair (y) direction. The negative (positive) N represents the electron (hole) carrier concentration.

10 Heat-energy conversion efficiency



SFig. 9: The calculated xx -component of η of PbCIF (left), PbBrF (middle), and PbIF (right) JLs as a function of hot-side temperature and carrier concentration n . In comparison, the PbCIF layer presents better Carnot efficiency at the carrier levels close to the Fermi level.



SFig. 10: The calculated xx -component of η for PbBrCl (left), PbICl (middle), and PbIBr (right) JLs as a function of hot-side temperature and carrier concentration n . In comparison, the PbCIF layer presents better Carnot efficiency at the carrier levels close to the Fermi level.

References

- [1] G. K. Madsen, J. Carrete, and M. J. Verstraete, *Comput. Phys. Commun.* **231**, 140 (2018).
- [2] A. E. Sudheer, G. Tejaswini, M. Posselt, and D. Murali, *Comput. Mater. Sci.* **243**, 113123 (2024).